Epigenetic regulation of *Il12* and *Il23* gene expression and autoimmune inflammation by the deubiquitinase Trabid

Jin Jin[1,2,*], **Xiaoping Xie**[2,*], **Yichuan Xiao**[2,4], **Hongbo Hu**[2,5], **Qiang Zou**[2], **Xuhong Cheng**[2], and **Shao-Cong Sun**[2,3]

[1]Life Sciences Institute, Zhejiang University, Hangzhou 310058, China

[2]Department of Immunology, The University of Texas MD Anderson Cancer Center, 7455 Fannin Street, Box 902, Houston TX 77030, USA

[3]The University of Texas Graduate School of Biomedical Sciences at Houston, Houston, Texas 77030, USA

[4]Institute of Health Sciences, Shanghai Institutes for Biological Sciences, Chinese Academy of Sciences and Shanghai Jiao Tong University School of Medicine, Shanghai 200031, China

[5]State Key Laboratory of Biotherapy, West China Hospital, Si-Chuan University and Collaborative Innovation Center for Biotherapy, Chengdu, 610041, P. R. China

Abstract

The proinflammatory cytokines interleukin 12 (IL-12) and IL-23 connect innate and adaptive immune responses and are also involved in autoimmune and inflammatory diseases. Here we describe an epigenetic mechanism of *Il12* and *Il23* gene regulation involving the deubiquitinase Trabid. Deletion of *Zranb1*, the gene encoding Trabid, in dendritic cells inhibited the induction of IL-12 and IL-23 expression by Toll-like receptors (TLR), impairing the differentiation of inflammatory T cells and protecting mice from autoimmune inflammation. Trabid facilitated TLR-induced histone modifications at the *Il12* and *Il23* promoters, which involved deubiquitination and stabilization of the histone demethylase Jmjd2d. These findings highlight an epigenetic mechanism of *Il12* and *Il23* gene regulation and establish Trabid as an innate immune regulator of inflammatory T cell responses.

Keywords

Trabid; Ubiquitination; IL-12; Jmjd2d; EAE

Innate immune cells, including dendritic cells (DCs) and macrophages, play an important role in regulating the nature and magnitude of adaptive immune responses[1]. They recognize microbial components via pattern-recognition receptors, including various toll-like receptors (TLRs), which trigger intracellular signaling events that induce the maturation and function of these cells. DCs function as the primary antigen-presenting cells required for activation of naïve T cells[2]. In addition, DCs and macrophages produce a plethora of cytokines that regulate CD4$^+$ T cell differentiation and promote inflammatory responses[3]. However, deregulated production of proinflammatory cytokines by innate immune cells also contributes to autoimmune and inflammatory diseases. The interleukin 12 (IL-12) family cytokines, particularly IL-12 and IL-23, are proinflammatory cytokines produced by dendritic cells, macrophages, as well as fibroblasts in response to microbial infections[4, 5, 6]. IL-12 is composed of the IL-12α and IL-12β subunits and acts as a key mediator of CD4$^+$ T cell differentiation towards T helper (T$_H$) 1 lineage characterized by production of a signature cytokine, interferon-γ (IFN-γ)[7]. IL-23, composed of IL-12β and a specific subunit, IL-23α, functions to amplify and maintain T$_H$17 subset of CD4$^+$ T cells[6, 7]. IL-12 and IL-23 are induced in response to stimulation by multiple TLR ligands and have been linked to autoimmune and inflammatory diseases[6]. However, the mechanism regulating the induction of *Il12* and *Il23* gene induction is incompletely understood.

The NF-κB transcriptional regulator c-Rel mediates TLR-stimulated expression of *Il12* and *Il23* genes[8, 9]. In addition to activating NF-κB and other transcription factors, TLR signals induce chromatin remodeling at the *Il12b* promoter, which may be important for the accessibility of the promoter region by specific transcription factors[10, 11]. As seen with the *Il12b* gene, chromatin remodeling allows the accessibility of the *Il12a* promoter by specific transcription factors, such as c-Rel and C/EBP[12]. Similarly, TLR stimulation results in histone modifications of the nucleosome located at the *Il23a* promoter[13, 14]. Each nucleosome contains the core histones H2A, H2B, H3 and H4, which are characteristically regulated by post-translational modifications including methylation and demethylation[15]. Recent work has indicated Jmjd2d as a demethylase that mediates histone 3 demethylation involved in *Il12b* induction in DCs[15, 16]. However, how Jmjd2d is regulated remains unclear.

Here we identified the deubiquitinase (DUB) Trabid (TRAF-binding protein domain, also known as Zranb1), as a crucial regulator of TLR-stimulated expression of IL-12 and IL-23. Trabid belongs to the OTU family of DUBs and preferentially hydrolyzes lysine 29 (K29)- and K33-linked ubiquitin chains[17, 18, 19]. *In vitro* studies using cancer cell lines suggest a role for Trabid in the regulation of Wnt signaling, but this function remains controversial[20, 21]. By employing a gene targeting approach, we show that Trabid deficiency in DCs and macrophages impaired the induction of *Il12* and *Il23* genes without affecting the induction of many other cytokine genes. Consistently, Trabid deficiency impaired the production of T$_H$1 and T$_H$17 subsets of inflammatory T cells, rendering mice refractory to the induction of experimental autoimmune encephalomyelitis (EAE), an autoimmune neuroinflammatory disease that is dependent on T$_H$1 and T$_H$17 cells. Our data suggest the involvement of an epigenetic mechanism, in which Trabid regulates histone modifications at the *Il12* promoter by controlling the fate of a histone demethylase, Jmjd2d.

RESULTS

Trabid is required for induction of EAE

To study the *in vivo* function of Trabid, we generated germline *Zranb1* knockout (called KO here throughout) mice and wild-type control mice by crossing *Zranb1*^{fl/fl} mice with CMV-Cre mice (**Supplementary Fig. 1a,b**). In addition, we crossed the *Zranb1*^{fl/fl} mice with *CD11c*-Cre and *Cd4*-Cre mice to generate DC-conditional *Zranb1* KO (*Zranb1*[f/f]*Cd11c*-Cre; called DC-cKO here throughout) and T-cell conditional *Zranb1* KO (*Zranb1*[f/f]*Cd4*-Cre; called T-cKO here throughout) mice, respectively (**Supplementary Fig. 1c,d**). The RT-PCR analyses revealed loss of *Zranb1* mRNA expression in T cells, B cells, DCs, and macrophages of the germline KO mice and in DCs and T cells of the DC-cKO and T-cKO mice, respectively (**Supplementary Fig. 1e**). The germline KO mice were born with expected Mendelian ratio, had normal growth and survival (data not shown) and did not show obvious abnormalities in thymocyte development, although they had a moderate reduction in the frequency of naïve T cells in the spleen (**Supplementary Fig. 2a,b**). The percentage of regulatory T (T_{reg}) cells among CD4$^+$ single-positive thymocytes and CD4$^+$ splenic T cells was comparable between wild-type and KO mice (**Supplementary Fig. 2c**). Additionally, deletion of Trabid had little or no effect on the frequency of conventional DCs or plasmacytoid DCs in the bone marrow and spleen (**Supplementary Fig. 2d**).

To investigate the function of Trabid in regulating immune responses, we employed a T cell-dependent autoimmunity model, EAE, which involves peripheral generation of central nervous system (CNS)-specific T_H1 and T_H17 subsets of inflammatory T cells and their subsequent migration to the CNS to induce inflammation and demyelination[22,23]. Wild-type mice immunized with the myelin oligodendrocyte glycoprotein (MOG) peptide MOG$_{35-55}$, along with pertussis toxin developed severe clinical symptoms (**Fig. 1a**), associated with profound immune cell infiltration and demyelination in the CNS (**Fig. 1b**). Compared to wild-type mice, KO mice displayed significantly delayed onset and reduced severity of EAE disease, as well as substantially less immune cell infiltration and demyelination in the CNS (**Fig. 1a,b**). Flow cytometry analyses revealed fewer CD4$^+$ and CD8$^+$ T cells and CD11b$^+$CD45^{hi} monocytes, both as frequency and absolute number in the CNS of KO mice compared to wild-type mice (**Fig. 1c**), along with increased frequency of CD11b$^+$CD45^{lo} microglia (**Fig. 1c**) during the effector phase of EAE. Consistent with reduced inflammatory cell infiltration, we detected reduced expression of the proinflammatory cytokine genes *Il6*, *Tnf*, *Il12a*, *Il12b*, and *Il23a* in the CNS of MOG$_{35-55}$-immunized KO mice compared to MOG$_{35-55}$-immunized wild-type mice (**Fig. 1d**), further suggesting attenuated induction of inflammation. In addition, the percentage of IL-17$^+$ T_H17 cells and IFN-γ^+ T_H1 cells within the CD4$^+$ T cells infiltrating the CNS was significantly reduced in the KO mice compared to wild-type (**Fig. 1e**). Compared to EAE-induced wild-type mice, EAE-induced KO mice also had a significantly lower frequency of T_H1 and T_H17 cells in the draining lymph nodes (**Fig. 1f**), and spleen (**Fig. 1g**), as determined by intracellular cytokine staining (**Fig. 1f**) and *in vitro* recall responses stimulated by the MOG peptide (**Fig. 1g**). These results suggest impaired generation of inflammatory T cells upon autoantigen immunization, highlighting a crucial role for *Trabid* in mediating *in vivo* T_H1 and T_H17 cell differentiation.

Trabid functions in DCs to regulate T cell differentiation

To determine if Trabid functions in T cells in a cell-intrinsic manner or regulates the CD4^{+} T cell responses through an effect on innate immune cells, particularly DCs, we induced EAE in T-cKO and DC-cKO mice. We found comparable EAE disease scores and CNS immune cell infiltration between wild-type and T-cKO mice immunized with MOG peptide (**Fig. 2a** and **Supplementary Fig. 3a**). In addition, EAE-induced T-cKO mice had no defects in the *in vivo* production of T_H1 and T_H17 cells or *in vitro* T cell recall responses to MOG peptide compared to wild-type mice (**Supplementary Fig. 3b,c**). Consistently, the *in vitro* differentiation efficiency of naïve T-cKO and wild-type CD4^{+} T cells into T_H1, T_H17, and T_{reg} cells was comparable (**Supplementary Fig. 3d**). Wild-type and Trabid-deficient naïve T cells also had similar capacity of proliferation and IL-2 and IFN-γ expression in response to *in vitro* TCR/CD28 stimulation (**Supplementary Fig. 3e,f**). These observations indicate a non-cell autonomous effect of Trabid in regulating T cell differentiation and EAE pathogenesis.

DCs play an important role in regulating the activation and differentiation of naïve CD4^{+} T cells[24]. Similar to KO mice, DC-cKO mice were refractory to EAE induction, which was associated with a profound reduction in the frequency and absolute number of CNS-infiltrating CD4^{+} T cells and CD11b^{+}CD45^{hi} myeloid cells (**Fig. 2b-d**) and a higher relative frequency of CNS-resident CD11b^{+}CD45^{lo} microglia (**Fig. 2c**), compared to wild-type mice. Intracellular cytokine staining revealed lower frequencies and absolute numbers of T_H1 and T_H17 cells, and lower numbers of T_{reg} cells, in the CNS of DC-cKO mice compared to wild-type mice following induction of EAE (**Fig. 2e**), corresponding to the overall reduction in immune cell infiltration into the CNS in these mice (**Fig. 2c,d**). We detected reduced frequency of T_H1 and T_H17 cells in the draining lymph nodes of DC-cKO mice (**Fig. 2e**) and reduced T_H1 and T_H17 cytokine recall responses in splenic DC-cKO T cells (**Fig. 2f**) compared to splenic wild-type T cells, suggesting impaired production of these inflammatory T cells. These data suggest that expression of Trabid in DCs regulated the generation of T_H1 and T_H17 cells and EAE pathogenesis.

MOG-immunized DC-cKO and wild-type mice had a similar frequency of CD11c^{+}CD11b^{+} DCs in the draining lymph nodes, which expressed comparable levels of the costimulatory molecules CD80 and CD86 (**Fig. 2g**), suggesting Trabid deletion did not affect DC development, migration or maturation. However, MOG-immunized DC-cKO mice had reduced expression of the inflammatory cytokine genes *Il6*, *Tnf*, *Il12a*, *Il12b*, and *Il23a* in the CNS (**Fig. 2h**) and reduced expression of *Il12a*, *Il12b* and *Il23a*, although not *Il6* and *Tnf*, in the draining lymph nodes (**Fig. 2h**) compared to MOG_{35-55}-immunized wild-type mice. Together, these observations suggested that Trabid might regulate T_H1 and T_H17 cell responses through IL-12 and IL-23 production in DCs.

Trabid regulates IL-12 and IL-23 expression downstream of TLRs

We next analyzed the effect of Trabid deficiency on TLR-stimulated DC activation and cytokine expression *in vitro*. Wild-type and DC-cKO bone marrow-derived DCs (BMDCs) expressed a similar level of the costimulatory molecules CD80 and CD86 following *in vitro* stimulation with the TLR4 ligand lipopolysaccharide (LPS; **Fig. 3a**) and displayed similar

capacity to mediate antigen-stimulated T cell proliferation, as determined based on CFSE dilution in co-cultured OT-II T cells (**Fig. 3b**). However, culture medium from LPS-stimulated DC-cKO BMDCs induced 2-3 fold lower differentiation of naïve $CD4^+$ T cells into T_H1 and T_H17 cells compared to conditioned medium from LPS-stimulated wild-type BMDCs (**Fig. 3c**). On the other hand, DC-cKO BMDCs induced T_{reg} cell differentiation similarly to wild-type BMDCs, either in the absence or presence of exogenous TGF-β (**Supplementary Fig. 4a**).

Real-time quantitative RT-PCR (qRT-PCR) detected significantly reduced expression of *Il12a*, *Il12b*, and *Il23a* mRNA, although similar expression of *Ifnb*, *Il1b*, *IL6*, *Tnf*, *Il10*, and *Nos2* mRNA, in DC-cKO BMDCs stimulated with LPS (**Fig. 3d**) or the TLR3 ligand poly(I:C) (**Fig. 3e**) compared to LPS- and poly(I:C)-induced wild-type BMDCs. Similar results were obtained by ELISA to assess the amount of secreted cytokines (**Fig. 3f**) and by qRT-PCR using FLT3 ligand-differentiated BMDCs stimulated with the TLR9 ligand CpG (**Fig. 3g**). Furthermore, exogenous IL-12 and IL-23 could rescue the defect of DC-cKO DCs in inducing T_H1 and T_H17 cell differentiation compared to wild-type DCs (**Supplementary Fig. 4b**). We also performed studies using bone marrow-derived macrophages (BMDMs) prepared from M-cKO mice and mouse embryonic fibroblasts (MEFs) prepared from Zranb1 germline KO mice. Compared to wild-type control cells, the M-cKO BMDMs and KO MEFs had reduced mRNA expression of *Il12* genes when stimulated with LPS (**Fig. 3h**) and lipofectamine-transfected poly(I:C) (**Fig. 3i**), respectively. Collectively, these results suggest that Trabid mediates induction of IL-12 and IL-23, thereby promoting T_H1 and T_H17 differentiation.

Trabid is required for recruitment of c-Rel to the *Il12* promoter

To elucidate the molecular mechanism by which Trabid mediates induction of IL-12 family of cytokines, we examined the role of Trabid in regulating TLR-mediated activation of MAP kinases (MAPKs), IκB kinase (IKK) and downstream transcription factors known to regulate *Il12* and *Il23* gene induction[25, 26, 27]. Compared to wild-type BMDCs, DC-cKO BMDCs did not show appreciable defect in LPS-stimulated phosphorylation of IKK and its substrates IκBα and p105 (**Fig. 4a**) or LPS-stimulated activation of the MAPKs p38, extracellular signal-regulated kinase (ERK), and c-Jun N-terminal kinase (JNK) (**Fig. 4b**). Furthermore, we observed similar levels of nuclear translocation of the NF-κB transcription factors c-Rel, p50, and p65, as well as CEBPβ and STAT3 in LPS-stimulated DC-cKO and wild-type BMDCs (**Fig. 4c**).

Because c-Rel has a very important role in the transcription of IL-12 cytokines [8, 9, 28], we used chromatin immunoprecipitation (ChIP) to examine whether Trabid regulated the TLR-stimulated recruitment of c-Rel to *Il12* gene promoters in DCs. Stimulation of wild-type BMDCs with LPS induced the binding of c-Rel in the promoter of *Il12b* gene, particularly between −220 and −16, a region known to contain an NF-κB-binding site (**Fig. 4d**), while c-Rel recruitment to this region was barely observed in DC-cKO BMDCs (**Fig. 4d**). Similar observations were made in BMDCs stimulated with CpG (**Fig. 4d**).

We also examined the recruitment of c-Rel to several other cytokine gene promoters that contain κB sites. LPS strongly induced the binding of c-Rel to the promoter of *Il12a* and *Il12b*, but not to that of *Ifnb*, in wild-type BMDCs, and the LPS-stimulated c-Rel recruitment to the *Il12a* and *Il12b* promoters was significantly reduced in DC-cKO BMDCs (**Fig. 4e** and **Supplementary Fig. 5a**). We found a low level of LPS-induced c-Rel binding to the *Il1b* promoter; however this occurred in both wild-type and DC-cKO BMDCs (**Supplementary Fig. 5a**). Another NF-κB member, p50, was recruited to both the *Il12* promoters and *Ifnb* promoter in LPS-stimulated wild-type BMDCs, and the recruitment of p50 to the *Il12* promoters, but not to the *Ifnb* promoter, was attenuated in DC-cKO BMDCs (**Fig. 4e**). Thus, although Trabid was dispensable for the nuclear translocation of NF-κB factors, it was required for recruiting c-Rel and p50 to *Il12* the promoters.

Trabid regulates histone modifications at the *Il12b* promoter

When transiently expressed in HEK293 cells, Trabid did not physically interact with c-Rel or inhibit c-Rel ubiquitination (data not shown), and it did not alter the transcriptional activity of c-Rel in a luciferase reporter assay (**Supplementary Fig. 5b**). We next investigated a possible epigenetic function for Trabid. Gene transcription and silencing are associated with active histone modifications, such as histone 3 lysine 4 trimethylation (H3K4me3), and repressive histone modifications, such as H3K9 dimethylation (H3K9me2) and trimethylation (H3K9me3), respectively[29,30,31]. We found that LPS induced H3K4me3, downregulated H3K9me2 and H3K9me3, and did not appreciably alter H3K27me3, in the *Il12b* promoter of wild-type BMDCs (**Fig. 5a**). Compared to wild-type BMDCs, the DC-cKO BMDCs had attenuated induction of H3K4me3 and significantly inhibited removal of the repressive histone marks, H3K9me2 and H3K9me3, in both the *Il12b* promoter (**Fig. 5a**) and the *Il12a* promoter (**Supplementary Fig. 5c**). Of note, *Rel* KO BMDCs did not show defect in the LPS-induced removal of H3K9me2 and H3K9me3 at the *Il12b* promoter compared to wild-type BMDCs (**Fig. 5b**), suggesting that these Trabid-dependent epigenetic changes were independent of c-Rel recruitment.

To assess the functional role of Trabid-mediated histone modifications at the *Il12* promoters, we determined the binding level of RNA polymerase II (Pol II) preinitiation complex components, including Pol II, serine-5 phosphorylated Pol II (Pol II pS5) and the general transcription factor subunits TFIIB and TFIID, in the *Il12/Il23* promoters. Compared to the wild-type BMDCs, the DC-cKO BMDCs had attenuated recruitment of these Pol II complex components to the TATA boxes of *Il12a*, *Il12b*, and *Il23a* promoters in response to LPS stimulation (**Supplementary Fig. 6**). In contrast, the wild-type and DC-cKO BMDCs did not show differences in LPS-stimulated recruitment of the Pol II complex components to the *Il1b* and *Il6* promoters (Supplementary Fig. 6). Collectively, these results suggest a role for Trabid in regulating TLR-induced histone modifications and assembly of RNA Pol II complex at the promoter of *Il12* genes.

The DUB activity of Trabid is required for its function

To determine whether the DUB catalytic activity of Trabid was required for *Il12* promoter regulation, we reconstituted *Zranb1* KO MEFs with a retroviral vector encoding wild-type Trabid or a catalytically inactive Trabid mutant (C443A). C443A Trabid showed similar, or

even more abundant, nuclear translocation as wild-type Trabid (**Fig. 5c**). However, wild-type Trabid, but not C443A Trabid, rescued the poly(I:C)+lipofectamine-induced removal of H3K9me2 and H3K9me3 (**Fig. 5d**) as well as the recruitment of c-Rel (**Fig. 5d**) at the *Il12b* promoter in KO MEFs. Consistently, reconstitution of KO MEFs with wild-type Trabid, but not C443A Trabid, greatly promoted poly(I:C)-induced *Il12b, Il12a* and *Il23a* mRNA expression in these cells (**Fig. 5e**) but had no effect on the induction of the control gene *Il6* (**Fig. 5e**). In similar experiments using BMDCs, reconstitution of DC-cKO BMDCs with wild-type Trabid, but not C443A Trabid, rescued the induction of *Il12a, Il12b*, and *Il23a* genes (**Fig. 5f,g**). Thus, the DUB catalytic activity of Trabid is essential for its function in the regulation of histone modifications and *Il12* gene induction.

Trabid regulates the demethylase Jmjd2d

We surmised that Trabid might regulate the ubiquitination of a factor involved in regulation of histone modification at the *Il12* promoter. In this regard, H2B monoubiquitination at K120 is known to promote H3 methylation[26]. However, although LPS upregulated H2B K120 monoubiquitination in wild-type BMDCs, a similar level of H2B K120 monoubiquitination was detected in DC-cKO cells (**Fig. 6a**). Because Jmjd2 demethylases have been shown to control removal of H3K9me2 and H3K9me3 histone marks[32], we screened all four Jmjd2 proteins using ChIP assays and found that LPS stimulation of wild-type BMDCs induced the binding of Jmjd2d, but not the other Jmjd2 members, to the *Il12b* promoter (**Fig. 6b and Supplementary Fig. 7a**). Furthermore, LPS-stimulated recruitment of Jmjd2d to the *Il12a* and *Il12b* promoters was largely lost in DC-cKO BMDCs compared to wild-type BMDCs (**Fig. 6b,c**). Jmjd2d was only weakly associated with the *Il1b* and *Il6* promoters in LPS-stimulated wild-type BMDCs, and this association was not inhibited in DC-cKO BMDCs (**Fig. 6c**). As seen with the inducible removal of H3K9me2/me3, the LPS-stimulated Jmjd2d recruitment to *Il12b* promoter was not affected by c-Rel deficiency (**Supplementary Fig. 7b**), consistent with the idea that chromotin modifications precede c-Rel recruitment.

We next examined the functional contribution of Jmjd2d to the induction of *Il12* genes. Incubation of wild-type BMDCs with a selective Jmjd2 inhibitor, 5-carboxy-8HQ, potently inhibited the LPS-stimulated expression of *Il12* and *Il23* genes, but not that of *Il1b* and *Il6* genes (**Fig. 6d**). Furthermore, 5-carboxy-8HQ had little or no effect on the induction *Il12* and *Il23* in DC-cKO BMDCs, consistent with the impaired promoter-recruitment of Jmjd2d in these mutant cells. Jmjd2d knockdown with two different shRNAs also led to significant inhibition of *Il12* and *Il23* gene induction in wild-type BMDCs (**Supplementary Fig. 7c,d**).

We next investigated the role of Trabid in regulating the ubiquitination and stability of Jmjd2d. The steady-state expression of Jmjd2d in wild-type BMDCs was low, but it was elevated upon LPS stimulation (**Fig. 6e**). However, the amount of Jmjd2d protein was only slightly increased following LPS stimulation in DC-cKO BMDCs (**Fig. 6e**). This phenotype was not due to altered expression of *Kdm4d* gene (encoding Jmjd2d), because LPS induced comparable amounts of *Kdm4d* mRNA in wild-type and DC-cKO BMDCs (**Fig. 6f**), indicating a posttranslational mechanism of Jmjd2d protein regulation. Indeed, treatment of LPS-stimulated DC-cKO BMDCs with the proteasome inhibitor MG132 restored the

amount of Jmjd2d protein to a level similar to that in LPS-stimulated wild-type BMDCs (**Fig. 6g**), suggesting that Trabid might stabilize Jmjd2d via deubiquitination. In support of this idea, wild-type Trabid, but not the catalytically inactive C443A Trabid mutant, stabilized Jmjd2d in poly(I:C)+lipofectamine-stimulated *Zranb1* KO MEFs (**Fig. 6h**). Furthermore, both wild-type and C443A Trabid physically associated with endogenous Jmjd2d in reconstituted KO MEFs (**Fig. 6i** and **Supplementary Fig. 7e**).

To directly examine the role of Trabid in regulating Jmjd2d ubiquitination, we analyzed the accumulation of ubiquitinated Jmjd2d in wild-type and DC-cKO BMDCs stimulated with LPS in the presence of the proteasome inhibitor MG132. DC-cKO BMDCs had markedly more abundant Jmjd2d ubiquitination than the wild-type BMDCs (**Fig. 6j**), suggesting that Trabid negatively regulated Jmjd2d ubiquitination. When transfected into HEK293 cells, wild-type Trabid, but not C443A Trabid, inhibited Jmjd2d ubiquitination (**Fig. 6k**), and the transfected Jmjd2d was abundantly conjugated with both K11- and K29-linked polyubiquitin chains (**Fig. 6l**). Consistent with prior *in vitro* findings that Trabid preferentially cleaves K29-linked ubiquitin chains[18, 19], transfected Trabid efficiently reduced the K29 ubiquitination of Jmjd2d (**Fig. 6l**), although Trabid also had an inhibitory effect on K11 ubiquitination of Jmjd2d, albeit more weakly than on K29 ubiquitination (**Fig. 6l**). Retroviral transduction of Jmjd2d in DC-cKO BMDCs increased the amount of Jmjd2d protein level in these cells (**Supplementary Fig. 7f**) and significantly increased the expression of *Il12a*, *Il12b*, and *Il23a* genes (**Supplementary Fig. 7g**). Collectively, these data suggest that in TLR-stimulated DCs Trabid deubiquitinates and stabilizes Jmjd2d, thereby regulating histone modifications and expression of *Il12a*, *Il12b*, and *Il23a* genes (**Supplementary Fig. 8**).

Discussion

The IL-12 family of cytokines plays a crucial role in the polarization of $CD4^+$ T cells to T_H1 and T_H17 cells and the pathogenesis of EAE[33]. In the present study, we identified the DUB Trabid as an essential regulator of *Il12* gene expression in both innate immune cells and fibroblasts. Trabid deficiency impaired TLR-stimulated expression of IL-12 and IL-23 *in vitro* and suppressed T cell polarization and EAE pathogenesis *in vivo*. Mechanistically, Trabid modulated the TLR-induced histone modifications at the promoter region of *Il12* genes.

Epigenetic factors play a crucial role in the regulation of *Il12* genes[34, 35, 36]. In particular, the histone demethylases Aof1 and Jmjd2d have been implicated in the removal of H3K9me2 and H3K9me3 from the *Il12b* promoter, thereby promoting stimulus-induced recruitment of transcription factors like c-Rel[16, 37]. Our data suggest a ubiquitin-dependent mechanism of Jmjd2d regulation. Along with its inducible synthesis in TLR-stimulated DCs, Jmjd2d underwent ubiquitination and proteolysis, which was counter-regulated by the deubiquitinase Trabid. Trabid deficiency promoted Jmjd2d degradation and inhibited the removal of the transcriptionally repressive histone marks, H3K9me2 and H3K9me3 at the promoter region of *Il12* genes. Trabid deletion also inhibited the induction of the transcriptionally active histone mark H3K4me3 at the promoter region of *Il12* genes. Previous studies have shown that H3K9 and H3K4 methylations are mutually regulated, with

H3K9 methylation inhibiting H3K4 methylation and vice versa[38]. It is thus possible that Trabid may regulate both types of histone methylation events via the same mechanism, although the involvement of two independent mechanisms cannot be excluded.

Our data suggest that Trabid is dispensable for TLR-stimulated c-Rel activation but is required for c-Rel recruitment to the promoter of *Il12* genes. It is likely that the promoter recruitment of c-Rel may rely on histone modifications, because these epigenetic events are also dependent on Trabid. In further support of this possibility, c-Rel was not required for TLR-stimulated Jmjd2d recruitment to the *Il12* promoter or the histone modification events. We noticed that Trabid regulated H3K9 di- and tri-methylations in a broad region of the *Il12b* locus, whereas c-Rel was specifically recruited to the promoter-proximal region of *Il12b* known to contain a κB enhancer. Thus, although histone modifications might promote c-Rel recruitment to the *Il12* promoter, the specificity of this latter event is likely guided by the κB enhancer. The molecular mechanism underlying the inducible recruitment of Jmjd2d to specific promoters is currently unclear.

A prior *in vitro* study using cancer cell lines suggests a role for Trabid in regulating TCF-mediated transcription in Wnt signaling pathway[20], although this function of Trabid has remained controversial [21]. Trabid has also been shown to interact with and inhibits K63 ubiquitination of *Drosophila* TAK1, reducing the expression of downstream genes encoding antimicrobial peptides in flies[42]. TAK1 is a master kinase that mediates activation of IKK and its downstream transcription factor NF-κB, as well as the activation of MAPKs[43]. We found that Trabid was dispensable for TLR-stimulated activation of IKK-NF-κB and MAPKs in mouse DCs. Consistently, Trabid deficiency did not affect the induction of various NF-κB-target genes, such as *Tnfa, Il1b* and *Il6* but led to specific defect in the induction of *Il12* genes. Such distinct activity by Trabid may be due to differences between insect and mammalian systems.

The connection between Trabid and Jmjd2d raises the question of whether Trabid regulates additional genes. While this question needs to be addressed in future studies, our current work revealed that Trabid was dispensable for the induction of several other genes, including *Ifnb*, *Tnf*, *Il1b*, *Il6*, *Il10* and *Nos2*. Our data further suggested that Trabid-mediated IL-12 and IL-23 induction plays an important role in mediating inflammatory T cell responses and the pathogenesis of EAE, an animal model of the autoimmune neuroinflammatory disease multiple sclerosis. These findings implicate Trabid and Jmjd2d as potential therapeutic targets for the treatment of inflammatory diseases, such as multiple sclerosis.

ONLINE METHODS

Mice

Zranb1-targeted mice(Zranb1$^{tm1a(EUCOMM)Hmgu}$) were generated at Knockout Mouse Project (KOMP) by targeting exon 3 of *Zranb1* gene using a FRT-LoxP vector (Supplementary Fig. 1a). *Zranb1*-floxed mice (in C57BL/6 × 129/Sv mixed background) were generated by crossing the *Zranb1*-targeted mice with FLP deleter mice (Rosa26-FLPe; Jackson Laboratory). The *Zranb1*-floxed mice were further crossed with CMV-Cre, *Cd4*-Cre, *Cd11c*-Cre, and *Lyz2*-Cre mice (all from Jackson Laboratory, C57BL/6 background) to

generate *Zranb1* germline KO, T-cKO (*Zranb1*^f/f^*Cd4*-Cre), DC-cKO (*Zranb1*^f/f^*Cd11c*-Cre), and M-cKO (*Trabid*^f/f^*Lyz2*-Cre) mice, respectively. Heterozygous mice were bred to generate littermate controls and KO (or conditional KO) mice for experiments. Outcomes of animal experiments were collected blindly and recorded based on ear-tag numbers of the experimental mice. Genotyping was performed as indicated in Supplementary Fig. 1. Mice were maintained in specific pathogen-free facility, and all animal experiments were conducted in accordance with protocols approved by the Institutional Animal Care and Use Committee of the University of Texas MD Anderson Cancer Center.

Antibodies, plasmids, and reagents

Antibodies used in immunoblotting, immunoprecipitation, and ChIP assays are listed in Supplementary Table 3. Fluorescence-labeled antibodies are described in the section of flow cytometry and cell sorting. Human Trabid cDNA was amplified by PCR from the pHM6-HA-Trabid plasmid (provided by Dr. Mariann Bienz, Medical Research Council, UK) and inserted into the pCLXSN(GFP) retroviral vector[44]. The catalytically inactive Trabid mutant, HA-Trabid C443A, was created by site-directed mutagenesis. Mouse Jmjd2d expression vector (pcDNA-FLAG-mKdm4d) was obtained from Addgene, and the cDNA insert was transferred to the pCLXSN(GFP) vector to generate pCLXSN(GFP)-HA-Jmjd2d. pGIPZ lentiviral vectors encoding a non-silencing shRNA control and two different Jmjd2d shRNAs were obtained from Thermo Scientific.

LPS (derived from Escherichia coli strain 0127:B8) and CpG (2216) were from Sigma-Aldrich. Poly (I:C) was from Amersham, and recombinant murine GM-CSF was from Peprotech. The Jmjd2 inhibitor 5-carboxy-8HQ was purchased from Tocris Bioscience.

Induction and assessment of EAE

For active EAE induction, age- and sex-matched mice were immunized s.c. with MOG_{35-55} peptide (300μg) mixed in CFA (Sigma-Aldrich) containing 5 mg/ml heat-killed Mycobacterium tuberculosis H37Ra (Difco). Pertussis toxin (200 ng, List Biological Laboratories) in PBS was administered i.v. on days 0 and 2. Mice were examined daily and scored for disease severity using the standard scale: 0, no clinical signs; 1, limp tail; 2, paraparesis (weakness, incomplete paralysis of one or two hind limbs); 3, paraplegia (complete paralysis of two hind limbs); 4, paraplegia with forelimb weakness or paralysis; 5, moribund or death. After the onset of EAE, food and water were provided on the cage floor. For visualizing CNS immune cell infiltration and demyelination, spinal cords of the EAE-induced mice were collected on day 30 and subjected to hematoxylin and eosin (H&E) and luxol fast blue (LFB) staining, respectively. Mononuclear cells were prepared from the CNS (brain and spinal cord) of EAE-induced mice as described[45] and analyzed by flow cytometry.

Flow cytometry, cell sorting, and intracellular cytokine staining

Single-cell suspensions of Spleen, bone marrow or brains and spinal cords from MOG_{35-55}-immunized mice were subjected to flow cytometry using FACSAria (BD Bioscience) and the following fluorescence-labeled antibodies from eBioscience: PB-conjugated anti-IFNγ, anti-CD4, and anti-CD11c; PE-conjugated anti-B220 and anti-IL-17A; APC-conjugated

anti-CD11b and anti-CD62L; APC-CY7-conjugated anti-CD8; and FITC-conjugated anti-CD44 and anti-Foxp3.

For intracellular cytokine staining, the CNS-infiltrating T cells were stimulated for 4 h with PMA plus ionomycin in the presence of monensin and then subjected to intracellular IFN-γ, IL-17A staining and flow cytometry analysis.

In vitro CD4+ T cell differentiation

Purified naïve CD4+ T cells (CD44loCD62Lhi) were activated with plate-bound anti-CD3 and anti-CD28 under Th0 (5 μg/ml anti-IL-4 and 5 μg/ml anti–IFN-γ), T_H1 (5 μg/ml anti–IL-4 and 10 ng/ml IL-12), T_H17 (5 μg/ml anti-IL-4, 5 μg/ml anti-IFN-γ, 20 ng/ml IL-6, and 2.5 ng/ml TGF-β), or T_{reg} cells (5 μg/ml anti-IL-4, 5 μg/ml anti-IFN-γ, and 1 ng/ml TGF-β) conditions. The concentration of anti-CD3 antibody was 5 μg/ml for Th0 and T_H1 conditions and 1 μg/ml for T_H17 and T_{reg} conditions, whereas the concentration of anti-CD28 was 1 μg/ml for all conditions. After 4 d of activation, T_{reg} cells were quantified by flow cytometry based on staining of Foxp3. For detection of T_H1 and T_H17 cells, the cells were restimulated for 4 h with PMA and ionomycin in the presence of a protein transport inhibitor, monensin, followed by intracellular staining of IFN-γ and IL-17, respectively.

Generation of BMDCs and BMDMs

Bone marrow cells isolated from the wild-type or DC-cKO mice were cultured in RPMI 1640 medium contained 10% FBS supplemented with GM-CSF (10 ng/ml) for 7 days. The differentiated BMDCs were stained with Pacific blue-conjugated anti-CD11c and isolated by FACS sorter. In some experiments, BMDCs were also generated using medium supplemented with FLT3 ligand (20 ng/ml). Other than stated, GM-CSF-differentiated BMDCs were used in the experiments. BMDMs were generated using MCSF-supplemented medium.

For retroviral infection of Trabid-deficient BMDCs, Retrovirus particles were produced by transfecting HEK293 cells (using calcium-phosphate method) with pCLXSN-(GFP)-HA-jmjd2d or pCLXSN-(GFP) control vector, along with the packaging vectors pCL-ampho and VSV-G. BMDCs, differentiated using GM-CSF-supplemented medium for 3 days, were infected with the recombinant retroviruses for 8 h and then continued cultured under GM-CSF-supplemented medium. After 5 days, the GFP positive cells were sorted by flow cytometry and used for experiments.

Functional assays of DCs *in vitro*

The function of DCs was measured based on their ability to mediate antigen-stimulated activation of the OVA-specific OTII cells. DCs isolated from wild-type or DC-cKO mice were incubated for 6 h with 5 mg/ml OVA after stimulated with LPS (100ng/ml) for 12h, washed for 3 times with fresh medium, and then mixed with naïve OTII CD4+ T cells (CD44loCD62Lhi) labeled with CFSE. After three days, flow cytometry was performed to measure the proliferation of OTII T cells based on CFSE dilution.

For functional examination of DC-secreted cytokines in regulating T cell differentiation, the wild-type and DC-cKO DCs were stimulated with LPS for 48 h, and the supernatants were collected for inducing T cells differentiation. Naïve CD4^{+} T cells (CD44^{lo}CD62L^{hi}) isolated from wild-type mice were stimulated for 4 days with plate-bound anti-CD3 (5μg/mL) and anti-CD28 (1μg/mL) plus the DC culture supernatants described above, followed by intracellular cytokine staining and flow cytometry to measure the frequency of IFN-γ-producing T_H1 cells and IL-17-producing T_H17 cells or the Foxp3^{+} T_{reg} cells. In some experiments, exogenous IL-12 and IL-23 were provided. Cytokine induction in DCs was also measured by ELISA and qRT-PCR.

Jmjd2d knockdown

Lentiviral particles were produced by transfecting HEK293 cells (using calcium-phosphate method) with a pGIPZ lentiviral vector, encoding either a non-silencing shRNA or Jmjd2d-specific shRNAs, along with the packaging vectors psPAX2 and pMD2. BMDCs, differentiated using GM-CSF-supplemented medium for 5 days, were infected with the lentiviruses for 8 h. After 72 h, the infected cells were enriched by flow cytometric cell sorting (based on GFP expression) and subsequently used for experiments.

ELISA and qRT-PCR

Supernatants of *in vitro* cell cultures were analyzed by ELISA using a commercial assay system (eBioScience). For qRT-PCR, total RNA was isolated using TRI reagent (Molecular Research Center, Inc.) and subjected to cDNA synthesis using RNase H-reverse transcriptase (Invitrogen) and oligo (dT) primers. qRT-PCR was performed in triplicates, using iCycler Sequence Detection System (Bio-Rad) and iQTM SYBR Green Supermix (Bio-Rad). The expression of individual genes was calculated by a standard curve method and normalized to the expression of *Actb*. The gene-specific PCR primers (all for mouse genes) are shown in Supplementary Table 1.

Immunoblotting, immunoprecipitation, and Ubiquitination assays

Whole-cell lysates or subcellular extracts were prepared and subjected to immunoblotting and immunoprecipitation assays as described[44]. For ubiquitination assays, cells were pretreated with MG132 for 2 h and then lysed with a Nonidet P-40 lysis buffer (50 mM Tris-HCl, pH7.5, 120 mM NaCl, 1% Nonidet P-40, 1 mM EDTA, 1 mM DTT) containing 6 M urea and protease inhibitors. Jmjd2d was isolated by IP with antibodies for Jmjd2d (93694, Abcam) and the ubiquitinated Jmjd2d was detected by immunoblotting using an anti-ubiquitin (P4D1). For transfection models, FLAG-Jmjd2d was transfected into HEK293 cells along with HA-ubiquitin or HA-ubiquitin mutants along with other indicated expression vectors, and the transfected cells were pretreated with MG132 for 2 h and then lysed for Jmjd2d IP followed by detecting ubiquitinated Jmjd2d by IB using anti-ubiquitin.

ChIP assays

ChIP assays were performed with DCs (6×10^7) stimulated for 6 h with LPS or MEFs (2×10^7) stimulated for 9 h with poly(I:C) plus lipofectamine. The cells were fixed with 1% formaldehyde and sonicated as previously described[46]. Lysates (from 2×10^7 cells in 3 ml)

were subjected to IP with the indicated antibodies, and the precipitated DNA was then purified by Qiaquick columns (Qiagen) and quantified by quantitative PCR (QPCR) using a pair of primers that amplify the target region of the indicated promoter (Supplementary Table 2). The precipitated DNA is presented as percentage of the total input DNA. For histone modification analyses, the DNA bound by modified histone 3 is presented as percentage of total histone 3-bound DNA. For all of the genes analyzed, the promoter region covering a well-defined κB site was selected for QPCR assays to analyze c-Rel recruitment and histone modifications. For examining recruitment of general transcription factor components, the TATA box region of the promoters was selected for ChIP assay QPCRs.

Luciferase reporter gene assays

HEK293 cells (2×10^5) were transfected, by calcium phosphate precipitation, with a firefly luciferase reporter driven by the *Il12b* promoter, along with the indicated cDNA expression vectors as well as the control pRL-TK promoter-driven Renilla luciferase reporter. At 36 h post-transfection, cells were collected for dual luciferase assays (Promega). Firefly luciferase activities were normalized based on the Renilla luciferase activities.

Statistical analysis

Statistical analysis was performed using Prism software. Kruskal-Wallis nonparametric test followed by Dunn's post analysis were performed for analysis of EAE scores and two-tailed unpaired t-tests were performed for all other data analyses. P values less than 0.05 were considered significant, and the level of significance was indicated as *P<0.05, **P<0.01. In the animal studies, 4 mice are required for each group based on the calculation to achieve a 2.3 fold change (effect size) in two-tailed t-test with 90% power and a significance level of 5%. All statistical tests are justified as appropriate, and data meet the assumptions of the tests. The variance is similar between the groups being statistically compared.

Supplementary Material

Refer to Web version on PubMed Central for supplementary material.

ACKNOWLEDGEMENTS

REFERENCES

1. Iwasaki A, Medzhitov R. Regulation of adaptive immunity by the innate immune system. Science. 2010; 327(5963):291–295. [PubMed: 20075244]

2. Ganguly D, Haak S, Sisirak V, Reizis B. The role of dendritic cells in autoimmunity. Nat Rev Immunol. 2013; 13(8):566–577. [PubMed: 23827956]

3. Merad M, Sathe P, Helft J, Miller J, Mortha A. The Dendritic Cell Lineage: Ontogeny and Function of Dendritic Cells and Their Subsets in the Steady State and the Inflamed Setting. Annual Review of Immunology. 2013; 31(1):563–604.

4. Trinchieri G. Interleukin-12 and the regulation of innate resistance and adaptive immunity. Nat Rev Immunol. 2003; 3(2):133–146. [PubMed: 12563297]

5. Gaffen SL, Jain R, Garg AV, Cua DJ. The IL-23-IL-17 immune axis: from mechanisms to therapeutic testing. Nat Rev Immunol. 2014; 14(9):585–600. [PubMed: 25145755]

6. Teng MWL, Bowman EP, McElwee JJ, Smyth MJ, Casanova J-L, Cooper AM, et al. IL-12 and IL-23 cytokines: from discovery to targeted therapies for immune-mediated inflammatory diseases. Nat Med. 2015; 21(7):719–729. [PubMed: 26121196]

7. Langrish CL, McKenzie BS, Wilson NJ, de Waal Malefyt R, Kastelein RA, Cua DJ. IL-12 and IL-23: master regulators of innate and adaptive immunity. Immunol Rev. 2004; 202:96–105. [PubMed: 15546388]

8. Sanjabi S, Hoffmann A, Liou HC, Baltimore D, Smale ST. Selective requirement for c-Rel during IL-12 P40 gene induction in macrophages. Proc Natl Acad Sci USA. 2000; 97(23):12705–12710. [PubMed: 11058167]

9. Hilliard BA, Mason N, Xu L, Sun J, Lamhamedi-Cherradi SE, Liou HC, et al. Critical roles of c-Rel in autoimmune inflammation and helper T cell differentiation. J Clinic Invest. 2002; 110:843–843.

10. Weinmann AS, Mitchell DM, Sanjabi S, Bradley MN, Hoffmann A, Liou H-C, et al. Nucleosome remodeling at the IL-12 p40 promoter is a TLR-dependent, Rel-independent event. Nat Immunol. 2001; 2(1):51–57. [PubMed: 11135578]

11. Weinmann AS, Plevy SE, Smale ST. Rapid and Selective Remodeling of a Positioned Nucleosome during the Induction of IL-12 p40 Transcription. Immunity. 1999; 11(6):665–675. [PubMed: 10626889]

12. Hayes MP, Murphy FJ, Burd PR. Interferon-gamma-dependent inducible expression of the human interleukin-12 p35 gene in monocytes initiates from a TATA-containing promoter distinct from the CpG-rich promoter active in Epstein-Barr virus-transformed lymphoblastoid cells. Blood. 1998; 91(12):4645–4651. [PubMed: 9616161]

13. Garrett S, Fitzgerald M, Sullivan KLPS, Poly I:C. Induce Chromatin Modifications at a Novel Upstream Region of the IL-23 p19 Promoter. Inflammation. 2008; 31(4):235–246. [PubMed: 18587636]

14. Mise-Omata S, Kuroda E, Niikura J, Yamashita U, Obata Y, Doi TS. A Proximal κB Site in the IL-23 p19 Promoter Is Responsible for RelA- and c-Rel-Dependent Transcription. The Journal of Immunology. 2007; 179(10):6596–6603. [PubMed: 17982049]

15. Bannister AJ, Kouzarides T. Regulation of chromatin by histone modifications. Cell Res. 2011; 21(3):381–395. [PubMed: 21321607]

16. Zhu Y, van Essen D, Saccani S. Cell-Type-Specific Control of Enhancer Activity by H3K9 Trimethylation. Molecular Cell. 2012; 46(4):408–423. [PubMed: 22633489]

17. Evans PC, Taylor ER, Coadwell J, Heyninck K, Beyaert R, Kilshaw PJ. Isolation and characterization of two novel A20-like proteins. Biochem J. 2001; 357:617–617. [PubMed: 11463333]

18. Licchesi JD, Mieszczanek J, Mevissen TE, Rutherford TJ, Akutsu M, Virdee S, et al. An ankyrin-repeat ubiquitin-binding domain determines TRABID's specificity for atypical ubiquitin chains. Nat Struct Mol Biol. 2012; 19(1):62–71. [PubMed: 22157957]

19. Virdee S, Ye Y, Nguyen DP, Komander D, Chin JW. Engineered diubiquitin synthesis reveals Lys29-isopeptide specificity of an OTU deubiquitinase. Nat Chem Biol. 2010; 6(10):750–757. [PubMed: 20802491]

20. Tran H, Hamada F, Schwarz-Romond T, Trabid Bienz M. a new positive regulator of Wnt-induced transcription with preference for binding and cleaving K63-linked ubiquitin chains. Genes Dev. 2008; 22:528–528. [PubMed: 18281465]

21. Shi T, Bao J, Wang N, Zheng J, Wu D. Identification Of Small Molecule TRABID Deubiquitinase Inhibitors By Computation-Based Virtual Screen. BMC Chemical Biology. 2012; 12(1):4. [PubMed: 22584113]

22. Peterson LK, Fujinami RS. Inflammation, Demyelination, Neurodegeneration and Neuroprotection in the Pathogenesis of Multiple Sclerosis. Journal of neuroimmunology. 2007; 184(1-2):37–37. [PubMed: 17196667]

23. Zepp J, Wu L, Li X. IL-17 receptor signaling and T helper 17-mediated autoimmune demyelinating disease. Trends Immunol. 2011; 32(5):232–239. [PubMed: 21493143]

24. Lanzavecchia A, Sallusto F. Regulation of T Cell Immunity by Dendritic Cells. Cell. 2001; 106(3): 263–266. [PubMed: 11509174]

25. Feng GJ, Goodridge HS, Harnett MM, Wei XQ, Nikolaev AV, Higson AP, et al. Extracellular signal-related kinase (ERK) and p38 mitogen-activated protein (MAP) kinases differentially regulate the lipopolysaccharide-mediated induction of inducible nitric oxide synthase and IL-12 in macrophages: Leishmania phosphoglycans subvert macrophage IL-12 production by targeting ERK MAP kinase. J Immunol. 1999; 163:6403–6403. [PubMed: 10586030]

26. Kim L, Rio LD, Butcher BA, Mogensen TH, Paludan SR, Flavell RA, et al. p38 MAPK Autophosphorylation Drives Macrophage IL-12 Production during Intracellular Infection. The Journal of Immunology. 2005; 174(7):4178–4184. [PubMed: 15778378]

27. Cho Y-C, Lee S, Lee M, Kim H, Oak M-h, Lee I-S, et al. Enhanced IL-12p40 production in LPS-stimulated macrophages by inhibiting JNK activation by artemisinin. Arch Pharm Res. 2012; 35(11):1961–1968. [PubMed: 23212638]

28. Sanjabi S, Williams KJ, Saccani S, Zhou L, Hoffmann A, Ghosh G, et al. A c-Rel subdomain responsible for enhanced DNA-binding affinity and selective gene activation. Genes Dev. 2005; 19(18):2138–2151. [PubMed: 16166378]

29. Zhang Y, Reinberg D. Transcription regulation by histone methylation: interplay between different covalent modifications of the core histone tails. Genes & Development. 2001; 15(18):2343–2360. [PubMed: 11562345]

30. Cedar H, Bergman Y. Linking DNA methylation and histone modification: patterns and paradigms. Nat Rev Genet. 2009; 10(5):295–304. [PubMed: 19308066]

31. Snowden AW, Gregory PD, Case CC, Pabo CO. Gene-Specific Targeting of H3K9 Methylation Is Sufficient for Initiating Repression In Vivo. Current Biology. 2014; 12(24):2159–2166. [PubMed: 12498693]

32. Cloos PAC, Christensen J, Agger K, Helin K. Erasing the methyl mark: histone demethylases at the center of cellular differentiation and disease. Genes & Development. 2008; 22(9):1115–1140. [PubMed: 18451103]

33. Kroenke MA, Carlson TJ, Andjelkovic AV, Segal BM. IL-12- and IL-23-modulated T cells induce distinct types of EAE based on histology, CNS chemokine profile, and response to cytokine inhibition. J Exp Med. 2008; 205:1535–1535. [PubMed: 18573909]

34. Wen H, Dou Y, Hogaboam CM, Kunkel SL. Epigenetic regulation of dendritic cell-derived interleukin-12 facilitates immunosuppression after a severe innate immune response. Blood. 2008; 111(4):1797–1804. [PubMed: 18055863]

35. Zhou L, Nazarian AA, Xu J, Tantin D, Corcoran LM, Smale ST. An Inducible Enhancer Required for Il12b Promoter Activity in an Insulated Chromatin Environment. Molecular and cellular biology. 2007; 27(7):2698–2712. [PubMed: 17242186]

36. Xu J, Pope SD, Jazirehi AR, Attema JL, Papathanasiou P, Watts JA, et al. Pioneer factor interactions and unmethylated CpG dinucleotides mark silent tissue-specific enhancers in embryonic stem cells. Proceedings of the National Academy of Sciences. 2007; 104(30):12377–12382.

37. van Essen D, Zhu Y, Saccani S. A feed-forward circuit controlling inducible NF-kappaB target gene activation by promoter histone demethylation. Mol Cell. 2010; 39(5):750–760. [PubMed: 20832726]

38. Fischle W, Wang Y, Allis CD. Histone and chromatin cross-talk. Curr Opin Cell Biol. 2003; 15(2): 172–183. [PubMed: 12648673]

39. Gallagher KA, Joshi A, Carson WF, Schaller M, Allen R, Mukerjee S, et al. Epigenetic Changes in Bone Marrow Progenitor Cells Influence the Inflammatory Phenotype and Alter Wound Healing in Type 2 Diabetes. Diabetes. 2015; 64(4):1420–1430. [PubMed: 25368099]
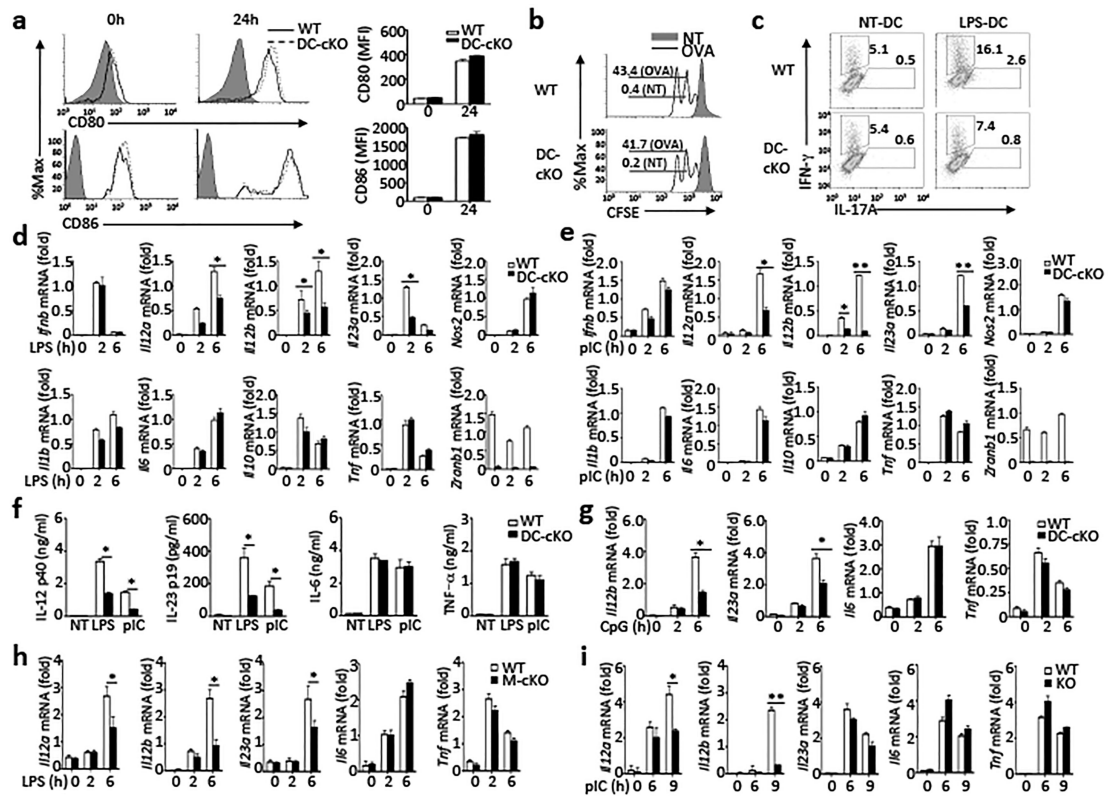
40. Xu P, Duong DM, Seyfried NT, Cheng D, Xie Y, Robert J, et al. Quantitative proteomics reveals the function of unconventional ubiquitin chains in proteasomal degradation. Cell. 2009; 137(1): 133–145. [PubMed: 19345192]

41. Dammer EB, Na CH, Xu P, Seyfried NT, Duong DM, Cheng D, et al. Polyubiquitin Linkage Profiles in Three Models of Proteolytic Stress Suggest the Etiology of Alzheimer Disease. Journal of Biological Chemistry. 2011; 286(12):10457–10465. [PubMed: 21278249]

42. Fernando MDA, Kounatidis I, Ligoxygakis P. Loss of Trabid, a New Negative Regulator of the *Drosophila* Immune-Deficiency Pathway at the Level of TAK1, Reduces Life Span. PLoS genetics. 2014; 10(2):e1004117. [PubMed: 24586180]

43. Mihaly SR, Ninomiya-Tsuji J, Morioka S. TAK1 control of cell death. Cell Death Differ. 2014

44. Reiley W, Zhang M, Wu X, Graner E, Sun S-C. Regulation of the deubiquitinating enzyme CYLD by IkappaB kinase gamma-dependent phosphorylation. Mol Cell Biol. 2005; 25:3886–3886. [PubMed: 15870263]

45. Jin W, Zhou XF, Yu J, Cheng X, Sun SC. Regulation of Th17 cell differentiation and EAE induction by the MAP3K NIK. Blood. 2009; 113:6603–6603. [PubMed: 19411637]

46. Nelson JD, Denisenko O, Bomsztyk K. Protocol for the fast chromatin immunoprecipitation (ChIP) method. Nat Protoc. 2006; 1(1):179–185. [PubMed: 17406230]
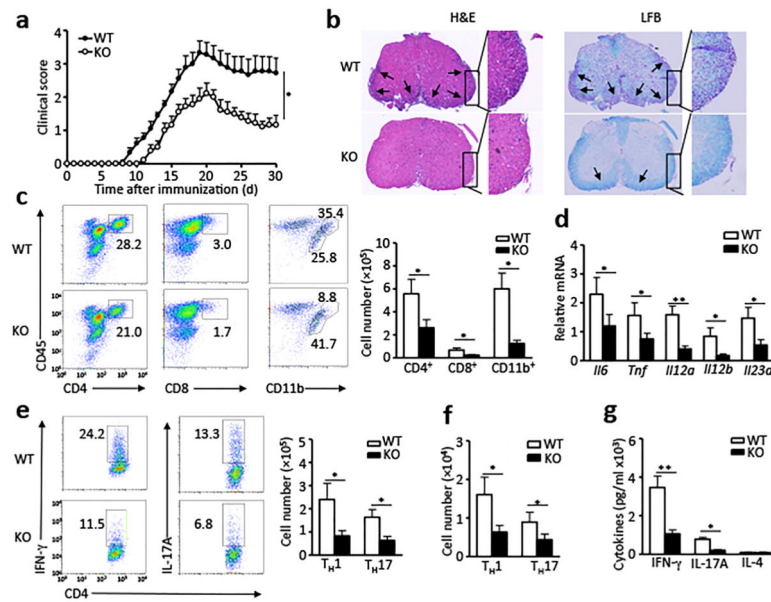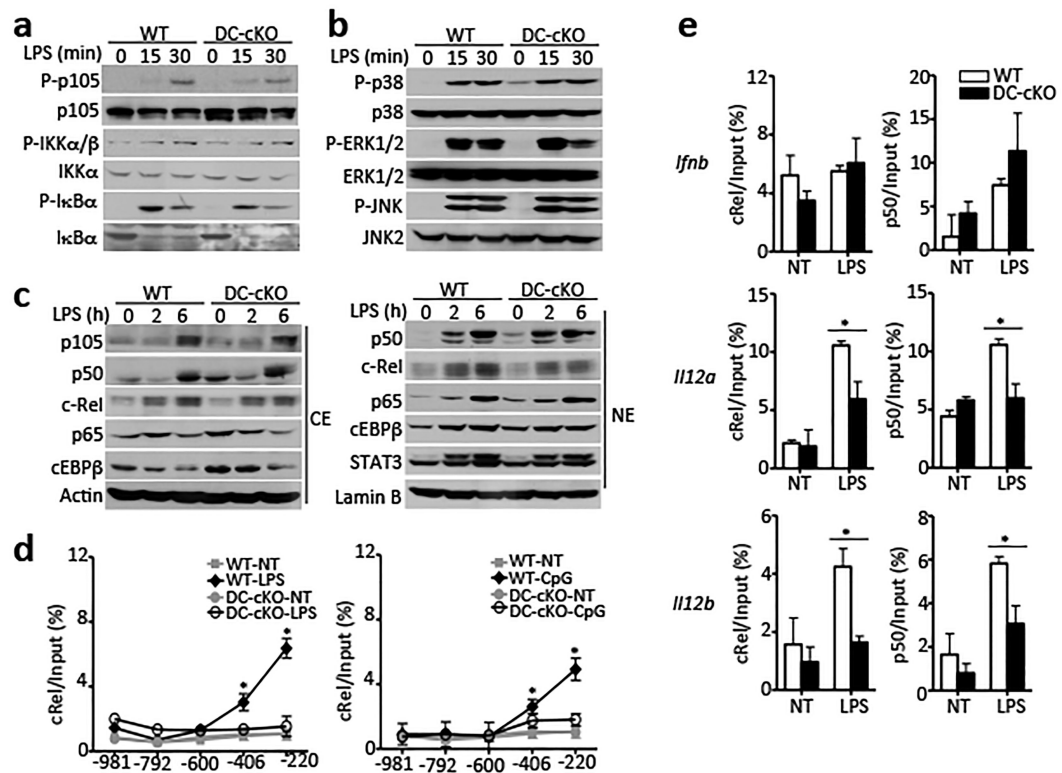
Figure 1.

Trabid-deficient mice are resistant to CNS inflammation. (**a**) Mean clinical scores of age- and sex-matched wild-type and *Zranb1* germline KO (KO) mice subjected to MOG$_{35-55}$-induced EAE (n=12/group). (**b**) H&E and luxol fast blue (LFB) staining of spinal cord sections from MOG$_{35-55}$-immunized wild-type and KO EAE mice for visualizing immune cell infiltration and demyelinization, respectively (arrows). Original magnification, ×100. (**c**) Flow cytometry analysis of immune cells (CD45$^+$) infiltrated into the CNS (brain and spinal cord) of MOG$_{35-55}$-immunized wild-type and KO mice (n = 3, day 14 post-immunization), presented as a representative plot (left) and summary graph of absolute cell numbers (right). (**d**) qRT-PCR analysis of indicated mRNAs in spinal cords of MOG$_{35-55}$-immunized wild-type and KO mice (n = 3, day 14 post-immunization). Data were presented as fold relative to the *Actb* mRNA level. (**e,f**) Flow cytometry analysis of T$_H$1 and T$_H$17 cells in the CNS (**e**) and draining lymph nodes (**f**) of MOG$_{35-55}$-immunized wild-type and KO mice (n = 3, day 14 post-immunization). Data are presented as a representative plot (left) and summary graph of the absolute cell numbers (right). (**g**) Splenocytes isolated from wild-type and KO EAE mice were restimulated for 48 h *in vitro* with MOG peptide (20 µg/ml), and supernatants were subjected to ELISA of the indicated cytokines. Data are representative of two (**a**, **b**) or three (**c-g**) independent experiments. Error bars are mean±SEM values. *P < 0.05; **P < 0.01 (Kruskal-Wallis nonparametric test (**a**) and two-tailed unpaired t-tests (**c-g**)).
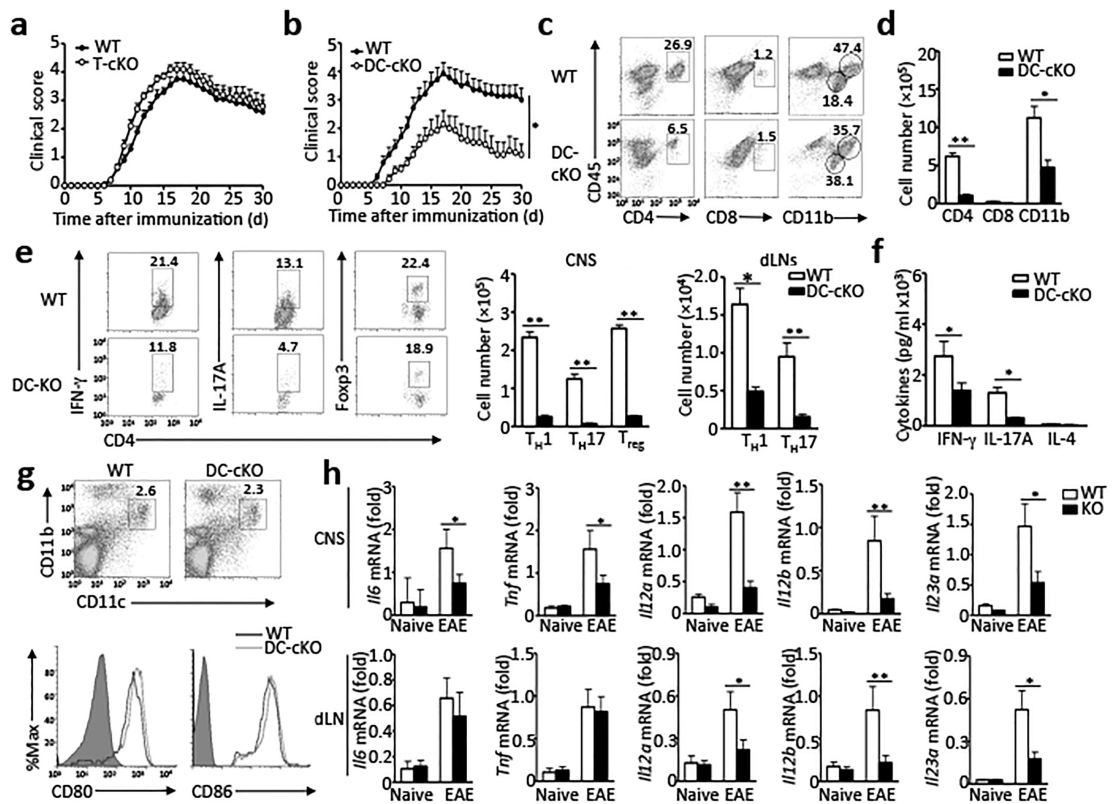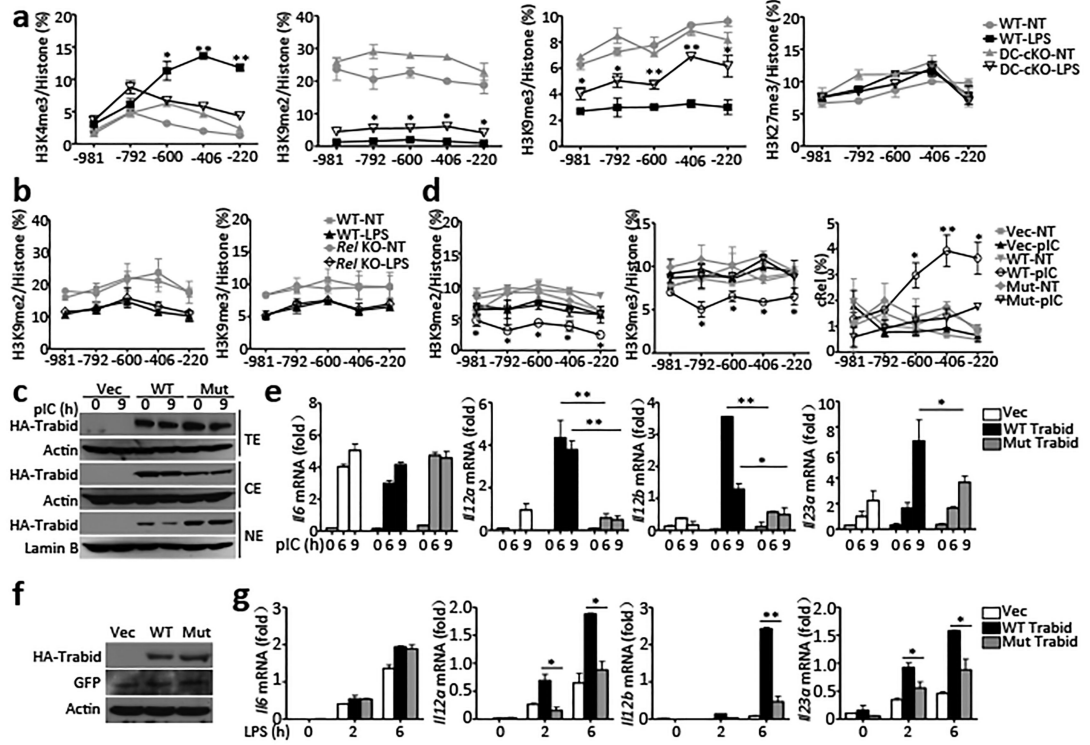
Figure 2.
Trabid is dispensable in T cells and crucial in DCs for EAE induction. (**a,b**) Mean clinical scores of T-cKO (**a**) and DC-cKO (**b**) mice or their age- and sex-matched wild-type control mice subjected to MOG$_{35-55}$-induced EAE (n=10/group). (**c,d**) Flow cytometry analysis of immune cell populations (CD45$^+$) infiltrated into the CNS (brain and spinal cord) of MOG$_{35-55}$-immunized wild-type and DC-cKO mice (n = 3, day 14 post-immunization), shown as a representative plot (**c**) and summary graph (**d**). (**e**) Flow cytometry analysis of TH1 and TH17 cells in the CNS and draining lymph nodes of MOG$_{35-55}$-immunized wild-type and DC-cKO mice (n = 3, day 14 post-immunization), shown as a representative plot (left, CNS cells) and summary graph (right). (**f**) ELISA of the indicated cytokines in culture supernatants of splenocytes isolated from wild-type and DC-cKO EAE mice (day 14 after MOG immunization) restimulated for 48 h with MOG peptide (20 μg/ml) in vitro. (**g**) Flow cytometry analysis of the frequency (upper) and costimulatory molecule expression (lower) of draining lymph node DCs of MOG$_{35-55}$-immunized wild-type and DC-cKO mice (n = 3, day 14 post-immunization). (**h**) qRT-PCR analysis of the indicated mRNAs (relative fold to *Actb*) in CNS or draining lymph nodes (dLN) of unimmunized (Naive) or MOG$_{35-55}$-immunized (EAE) wild-type and DC-cKO mice (n = 3, day 14 post-immunization). Data are representative of two (**a,b**) or three (**c-h**) independent experiments. Error bars are mean ±SEM values. *P < 0.05; **P < 0.01 (Kruskal-Wallis nonparametric test (**b**) and two-tailed unpaired t-tests (**d-f,h**)).

Figure 3.
Trabid is required for induction of IL-12 and IL-23 in innate immune cells. (**a**) Flow cytometry analysis of costimulatory molecule expression on untreated (0 h) or LPS-stimulated (24 h) wild-type and DC-cKO BMDCs, presented as a representative plot (left) and a summary graph of mean fluorescence intensity (MFI, right). (**b**) Proliferation analysis, based on flow cytometric measure of CFSE dilution, of CFSE-labeled naïve OTII CD4$^+$ T cells stimulated for 3 days with OVA-pulsed wild-type or DC-cKO BMDCs. (**c**) Flow cytometry analysis of IFN-γ-producing T_H1 cells and IL-17-producing T_H17 cells in wild-type naive CD4$^+$ T cells stimulated for 4 days with plate-bound anti-CD3 and anti-CD28 plus supernatants of wild-type or DC-cKO BMDC cultures that were either not treated (NT-DC) or stimulated with LPS for 48 h (LPS-DC). (**d,e**) qRT-PCR analysis of the indicated genes using wild-type or DC-cKO BMDCs stimulated with LPS (**d**) or poly(I:C) (**e**). Data are presented as fold relative to the *Actb* mRNA level. (**f**) ELISA of the indicated cytokines in supernatants of wild-type or DC-cKO BMDCs either not treated (NT) or stimulated with the indicated inducers for 24 h. (**g**) qRT-PCR analysis of the indicated genes using CpG-stimulated Flt3L-generated BMDCs. (**h,i**) qRT-PCR analysis of the indicated genes using LPS-stimulated wild-type and M-cKO BMDMs (**h**) or poly(I:C)/Lipofectamine-stimulated wild-type and KO MEFs (**i**). Data are mean ± SEM values and representative of at least three independent experiments. *P < 0.05; **P < 0.01 (two-tailed unpaired t-tests).
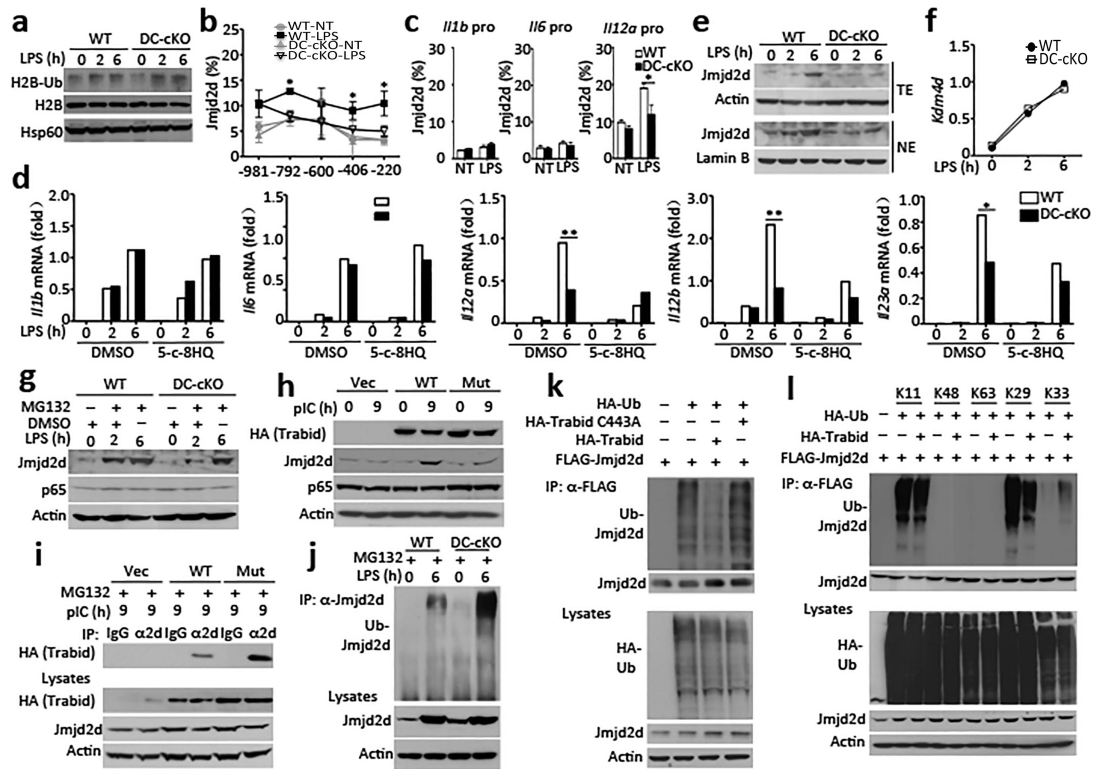
Figure 4.
Trabid is dispensable for TLR-stimulated signaling but is important for c-Rel recruitment to *Il12* promoters. (**a-c**) Immunoblotting analysis of the indicated phosphorylated (P-) and total proteins in whole-cell lysates (**a,b**) or cytoplasmic (CE) and nuclear (NE) extracts (**c**) of wild-type and DC-cKO BMDCs stimulated with LPS for the indicated time periods. (**d**) ChIP assays of c-Rel recruitment to different regions of *Il12b* locus wild-type or DC-cKO DCs that were untreated (NT) or stimulated with LPS or CpG for 6 h. The definitions of the different regions are −220, −220 to −16; −406, −406 to −193; −600, −600 to −395; −792, −792 to −584; and −981, −981 to −780. Statistical analyses compare the groups of LPS-stimulated wild-type and DC-cKO cells. (**e**) ChIP analysis of c-Rel and p50 binding to the indicated promoters in untreated (NT) or LPS-stimulated (6 h) wild-type and DC-cKO BMDCs. Data are presented as percentage based on total input DNA quantified by QPCR. Data are presented as mean ± SEM values of the percentage of c-Rel-bound DNA over total input DNA and representative of at least three independent experiments. Statistical analyses represent variations in technical replicates. *P < 0.05 (two-tailed unpaired t-tests).

Figure 5.
Trabid functions as a DUB to facilitate histone demethylation at the *Il12b* promoter and induction of *Il12* gene expression. (**a,b**) ChIP assays of histone modifications at the indicated regions of the *Il12b* promoter in untreated (NT) and LPS-stimulated (6 h) DC-cKO (**a**), *Rel* KO (**b**), or wild-type (WT) BMDCs. Statistical analyses compare the groups of LPS-stimulated wild-type and DC-cKO cells. (**c**) Immunoblotting analysis of the indicated proteins in total (TE), cytoplasm (CE), or nuclear (NE) extracts of KO MEFs reconstituted with pCLXSN(GFP) (Vec) or pCLXSN(GFP) encoding HA-tagged Trabid wild-type (WT) or C443A mutant (Mut), either untreated (0 h) or stimulated with lipofectamine-delivered poly(I:C) for 9 h. (**d,e**) ChIP assays of histone modifications and c-Rel recruitment at the indicated regions of *Il12b* promoter (**d**) and qRT-PCR analysis of the indicated genes (**e**) in reconstituted KO MEFs described in **c**, either untreated (NT) or stimulated with lipofectamine-delivered poly(I:C) for 9 h (**d**) or for the indicated times (**e**). Statistical analyses compare the groups of wild-type Trabid- and mutant Trabid-reconstituted MEFs stimulated with poly(I:C). (**f,g**) Immunoblotting (**f**) and qRT-PCR (**g**) assays using KO BMDCs reconstituted with pCLXSN(GFP) vector (Vec) or pCLXSN(GFP) encoding HA-tagged Trabid wild-type or C443A mutant, either untreated (**f**) or stimulated with LPS as indicated (**g**). Data are presented as mean ± SEM values and representative of at three independent experiments. Statistical analyses represent variations in technical replicates. *P < 0.05; **P < 0.01 (two-tailed unpaired t-tests).

Figure 6.
Trabid regulates the stability and function of Jmjd2d. (**a**) Immunoblotting of K120 monoubiquitinated H2B (H2B-Ub), total H2B, and Hsp60 in lysates of wild-type (WT) or DC-cKO BMDCs. (**b,c**) ChIP assays of Jmjd2d binding to different regions of *Il12b* promoter (**b**) or the indicated promoters (**c**) in untreated (NT) and LPS-stimulated (6 h) wild-type or DC-cKO BMDCs. Statistical analyses in **b** compare LPS-stimulated wild-type and DC-cKO cells. (**d**) qRT-PCR analysis using BMDCs pretreated for 12 h with 5-carboxy-8HQ (20 μM) or DMSO and then stimulated with LPS. (**e,f**) Immunoblotting using total-cell (TE) or nuclear (NE) extracts (**e**) and qRT-PCR (**f**) of LPS-stimulated wild-type or DC-cKO BMDCs. (**g,h**) Immunoblotting using whole-cell lysates of indicated BMDCs stimulated with LPS with MG132 or DMSO added (+) during last 2 h (**g**) or lysates of reconstituted MEFs (described in **Fig. 5c**) stimulated with lipofectamine-delivered poly(I:C). (**i**) Immunoblotting of HA-Trabid in immunoprecipitates of anti-Jmjd2d (α2d) or control IgG (top panel) and the indicated proteins in cell lysates (lower panels) of reconstituted KO MEFs, stimulated with lipofectamine-delivered poly(I:C) (MG132 added during last 2 h). (**j**) Immunoblotting of ubiquitinated Jmjd2d in anti-Jmjd2d immunoprecipitates and Jmjd2d and Actin in cell lysates of wild-type and DC-cKO BMDCs stimulated with LPS (MG132 added during last 2 h). (**k,l**) Immunoblotting of ubiquitinated Jmjd2d (using anti-ubiquitin) in anti-FLAG (Jmjd2d) immunoprecipitates (top panel) and of total cellular polyubiquitination (Poly-Ub), Jmjd2d, and Actin in lysates of HEK293 cells transfected with HA-tagged ubiquitin (**k**) or the indicated ubiquitin mutants (**l**) in the presence (+) or absence (−) of the indicated expression plasmids. Data are representative of three independent experiments. *P < 0.05; **P < 0.01 (two-tailed unpaired t-tests).